Maximum Energy Absorbed from the Persian Gulf Waves Considering Uncertainty in Power Take off Parameters

Mohammad Jalali[1], Reihaneh Kardehi Moghaddam[2*], Naser Pariz[3]
1- Department of Electrical Engineering, Mashhad Branch, Islamic Azad University, Mashhad, Iran.
Email: jalali.mohamad990@gmail.com
2- Department of Electrical Engineering, Mashhad Branch, Islamic Azad University, Mashhad, Iran.
Email: rkardehi.moghaddam@gmail.com (Corresponding author)
3- Department of Electrical Engineering, Ferdowsi University of Mashhad, Mashhad, Iran.
Email: n-pariz@um.ac.ir

Received: January 2021 Revised: March 2021 Accepted: July 2021

ABSTRACT:
Nowadays, sea wave energy is widely regarded as an energy source that is clean, renewable and highly available for power extraction. The subject of extracting the maximum power from sea waves in Iran is of great importance due to access to the Caspian Sea and the Persian Gulf. Moreover, there is a need for resources with no air pollution besides providing a part of the country's power demand without costly infrastructure, so this research field is highly interesting although has rarely been addressed so far. The main purpose of this paper is to use an appropriate control strategy to improve the performance of point absorbers. In this scheme, to consider high uncertainty in the parameters of the power take-off system in different atmospheric conditions and improve controller performance, a new improved black hole algorithm is introduced to tune fuzzy controller parameters. The proposed method is then implemented for tuning the fuzzy controller parameters in order to obtain the maximum power capture of wave energy converters. Compared to particle swarm optimization and conventional black hole algorithm, the results of the proposed method indicate enhancements in reference velocity tracking and absorbed power. Finally, some simulations are performed and the proposed controller is implemented for the wave spectrum of the Persian Gulf waters, so the performance of the proposed controller is evaluated.

KEYWORDS: Interval Type-2 Fuzzy Controller, Black Hole, Point Absorber; Uncertainty, Persian Gulf.

1. INTRODUCTION

Energy has always been a major determining factor in the social and economic development of countries. The population of the world is growing, so do the energy demand and power consumption. According to the outlook of the International Energy Agency, energy demand is expected to rise by about 70% until 2050. Thus, many countries have been investing in renewable energy as an alternative to limited energy resources such as fossil fuels to handle the potential crisis in the future. Among renewable energies, wave energy has the highest density and is considered as an alternative energy source for the future.

New technologies are being developed for harnessing wave energy. Accordingly, it is of great importance to choose the right location for wave energy converters. A Wave Energy Converter (WEC) extracts electrical energy from the sea/ocean wave mechanical energy.

Conventional WECs are passive controllers based on the principle of impedance matching. These converters match the resonant frequency of the WEC with the dominant frequency of the incident ocean waves [1] .A latching control in a converter locks the motion of the floating body exactly when its velocity vanishes at the end of one oscillation and then releases the body after a waiting, which is called the latching time. In this way, the velocity and excitation force are in phase and the absorbed power is maximized [2, 3].

Many researches are done for control of WEC converters. In [4], a simple control strategy was proposed to control the phase of a point absorber in irregular waves. This absorber uses a high-pressure hydraulic circuit and a battery. In [5], a quasi-spectral control scheme was studied to describe four basic

Paper type: Research paper
DOI: https:// 10.30486/mjee.2022.696491
How to cite this paper: M. Jalali, R. Kardehi Moghaddam and N. Pariz,“ **Maximum Energy Absorbed From the Persian Gulf Waves Considering Uncertainty in Power Take off Parameters**”, Majlesi Journal of Electrical Engineering, Vol. 16, No. 2, pp. 1-19, 2022.

components of such a control scheme, which includes reference generation calculations, tracking loop, wave excitation estimation and forecasting. In [6], a new mathematical tool called moment- adaptive control or moment-based phasor transform was proposed to calculate the steady state of the system.

The main advantage of the adaptive controller is robustness. However, its computational volume costs is high and it has another drawback which is system depreciation due to fast update of parameters.

Li et al. [7] along with Fusco and Ringwood [8] showed that the problem of controlling WECs to maximize the output energy that can be formulated as a constrained optimal control problem. This has led to a special type of controller known as predictive controller.

The Particle Swarm Optimization (PSO) algorithm was applied for on-line optimization of the fuzzy membership functions. The self-tunable fuzzy logic controller was used along with the PSO algorithm to model the force required by the power take-off system based on the principle of maximum power transfer, so that this force was used by a linear generator to drive point absorbers.

In [3], an analysis of the interval Type-2 fuzzy logic controllers (T2FLCs) and their advantages over Type-1 fuzzy logic controllers were discussed. Type-2 fuzzy systems (T2FSs) have attracted the interest of researchers in recent decades for handling uncertainties, nonlinearities, complexity in solutions, problem approximations and generalization. However, the computational complexity has been the reason behind the underdevelopment of these systems. From the point of view of lower computational complexity, the interval type-2 fuzzy systems (IT2FSs) are the most commonly utilized fuzzy system [9, 10]. Five main components of T2FSs are fuzzifier, rule base, inference system, type-reducer and defuzzifier. Type-reducers have been categorized into two groups, i.e., iterative and non-iterative algorithms. In the first group, KM and enhanced KM (EKM) are the most common type reducers [4, 5, 6], yet both are computationally-intensive and iterative. The second group that includes non-iterative approaches, e.g., Nie-Tan (NT) [8] [11], has a simple closed form. In this paper, we use an enhanced iterative algorithm with stop condition (EIASC), which is a promising approach for quickly and accurately finding a centroid for the T2FS output. The IT2FSs are employed in numerous applications [12]. In [13], an IT2FS was used in robot control along with neural networks. In [14], this system was used in multi-objective nonlinear programming problems, and in [15], a chaotic time-series prediction was considered. Moreover, Ref. [16] considered the modeling and control of a mobile robot, and an interval type-2 Takagi–Sugeno (T–S) fuzzy model was used in [9] to model a tele-robotic system. Reference [10] examined the performance of a specific approximation of the type-2 fuzzy inference system, which is the shadowed type-2 fuzzy inference system. The reason for using this method is to reduce the computational cost and approximation of type-2 fuzzy inference systems.

In [17], a reactive control method of a wave energy converter using artificial neural networks is studied. In [18], a neural network-based power control method for direct-drive wave energy converters in irregular waves was proposed. The advantages of neural network are that, it is suitable for complex systems and it is suitable for problems with unknown dynamics, but the disadvantages of neural network are that learning the network may be difficult or even impossible, also accuracy of the results depends on the size of the training set.

Spring- resonance-assisted maximal power tracking control of a direct-drive wave energy converter using sliding mode control is studied by Wang et al in 2021 [19]. In [20], non-causal linear optimal control with adaptive sliding mode observer is used for multi-body wave energy converters. The advantage of sliding mode control is that, it is suitable for nonlinear systems and it is robust against disturbances. But it has phenomenon of chattering problem.

In this paper, the under-control system is a complex nonlinear non-affine system with two control inputs that are not multiplied by the state variables. Therefore, designing a controller for this system is a challenging task. To propose an optimal interval type-2 fuzzy controller that maximizes the absorbed power, three different tools are employed, i.e., a Model-Based Feedback Controller (MBFC), an Interval Type 2 Fuzzy Controller (IT2FC) for each input variable and a unified Black-Hole Optimization Algorithm (BHOA) for the entire closed-loop system. First, we utilize the existing knowledge about the system dynamics to design two MBFCs, each for each control input. This approach simplifies the dynamic model of the system and compensates for the known part of system equations of motion in an intelligent manner. These MBFCs reduce the complexity of a wave-energy converter system to some extent. To the best of our knowledge, this novel approach has never been used before in the literature. With this modification, the new system is much easier to design for an intelligent controller. Second, an IT2FC is proposed for each input to enhance the absorber performance by providing the remaining control signal. The IT2FCs have several advantages including a smooth output signal, a high degree of freedom and the proved general-approximator property. However, parameters of the proposed IT2FCs have to be determined subject to extracting the maximum power. To do so, a unified BHOA is utilized for both IT2FCs. Finally, a novel optimal IT2FC is introduced to maximize the power absorbed via a point wave-energy absorber.

One of the major problems that is ignored in most articles is the existence of several uncertainties that occur as an uncertain parameter in the proposed models for various types of wave energy absorbers, including mechanical parts erosion, limescale deposition and algae on buoyant which causes it to change weight. Ignoring these uncertainties will reduce the accuracy of the controller performance. Therefore, in this paper, for the first time, a fuzzy control process with optimized extracted rules and parameters is applied to control the damper and spring coefficients of the mechanical model describing power takeoff system, which not only uses fuzzy control properties but also covers uncertainties.

The remaining of this paper is organized as follows: Section 2 presents the structure of a point absorber WEC, the governing relations, and the operation principle of this device. Section 3 discusses the problem of wave energy control using a T2FLC and applying it to a point absorber WEC. Moreover, the mathematical relations governing this type of controller are presented in this section. The optimization of the controller parameters is conducted in Section 4 using the black hole algorithm. Section 5 evaluates the performance of the proposed design simulation and the proposed controller and calculates the maximum absorbed power in the Persian Gulf waters.

2. HYDRODYNAMIC MODEL OF A FLOATING POINT ABSORBER-TYPE WEC

Because of the nonlinear nature of the incident waves that affects the mechanism and control of the power take-off system, WECs are usually nonlinear devices. The time-domain model of a point absorber uses the interaction between the waves and the floater [13] . The forces acting on the converter are generally divided into two types. The first type includes the forces acting on the floater by the surrounding water, which are also known as the hydraulic forces. The second type includes the forces acting on the floater from other parts of the converter such as the PTO and spring forces. The governing equation for the motion of a floating WEC is derived from the Newton's second law as follows:

$$f_{ex}(t) - f_r(t) - f_b(t) - f_{loss}(t) - f_{rs}(t) + f_u(t) - f_m(t) - f_d(t) = m\ddot{z}(t) \quad (1)$$

Where m is the total mass of the buoyant , the connecting rod, and the permanent magnet linear generator. $\ddot{z}(t)$ is the acceleration of the buoyant , $f_{ex}(t)$ is the wave excitation force, $f_r(t)$ is the radiation force, $f_b(t)$ is hydrostatic buoyancy force, $f_{loss}(t)$ is the mechanical and hydrodynamic loss force, $f_{rs}(t)$ is the spring-like force, $f_u(t)$ is the mechanical control force exerted by the permanent magnet linear generator (power take-off system) ,due to the new power take off structure, it has variable and adjustable parameters, $f_m(t)$ is the nonlinear mooring force, used to hold the converter fixed and $f_d(t)$ is the nonlinear drag force. Fig. 1 illustrates the general structure of a point absorber. Table 1 presents the linear and nonlinear forces acting on the hydrodynamic model of a floating point absorber-type WEC.

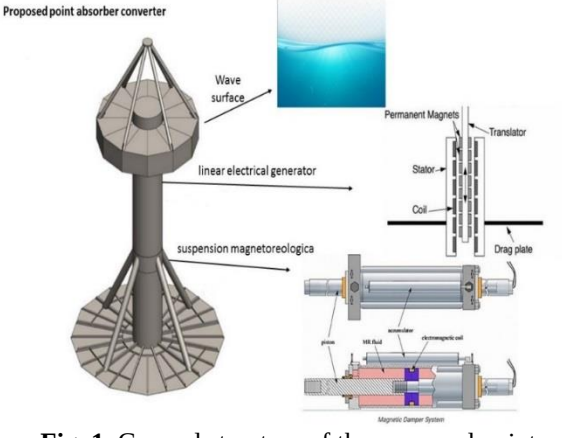

Fig. 1. General structure of the proposed point absorber.

Table 1. A list of linear and nonlinear forces acting on the hydrodynamic model of a WEC [21]**.**

force	Force formula	Description
$f_r(t)$	$f_r(t) = m_\infty \ddot{z} + \int_0^t k_r(t-\tau)\dot{z}(t)d\tau$	The hydrodynamic reflection force $f_r(t)$ is a force whose output is dependent only on the input values in the present and past (not the future), m_∞ is the mass added at infinite frequency, and the second term is estimated by a nonlinear model
$f_d(t)$	$f_d(t) = 0.5\ \rho\ A_w\ C_d\ \lvert\dot{z}(t)\rvert\dot{z}(t)$	Stretching force $f_d(t)$ is a force in which an object is pressurized by the movement of a fluid and into a nonlinear force.

$f_{ex}(t)$	$\int_0^t k_{ex}(t-\tau)\,{}^{\eta}f_{ex}(t) = K_{ex}(t) * {}^{\eta}(t) = (t)d\tau$	The hydrodynamic force applied by floating wave waves is considered as the main excitation force of the wave-converter system
$f_b(t)$	$f_b(t) = \rho g A_w z(t) = S_b z(t)$	The floating force is the force created by the difference between the floating body and the fluid weight .displaced during the oscillation
$f_u(t)$	$f_{\mathrm{u}} = -R_U(t)\dot{Z}(t) + S_U(t)Z(t)$	The controlled power of the boot system (pto) is entered into the converter and its task is to extract the maximum power.
$f_{rs}(t)$	$f_{rs}(t) = S_{rs}z(t)$	The linear force created by the springs between the floating body and the power system translator is below the water level
$f_{loss}(t)$	$f_{loss}(t) = R_{loss}\dot{z}(t)$	The force that results from the friction and non-ideal performance of the system
$f_m(t)$	$f_m(t) = 2S_m Z(t)(1 - l_m\sqrt{{l_m}^2 + z(t)^2})$	A nonlinear force that is used to keep the point absorber WEC in place.

By inserting all linear and nonlinear forces, the dynamics of the system in Fig. 1 is obtained. Assuming that

$$M^{-1} = \frac{1}{\mathrm{m}+\mathrm{m}_\infty} \tag{2}$$

we have

$$\begin{cases} \ddot{\mathrm{z}}(\mathrm{t}) = \mathrm{M}^{-1}\left(\mathrm{f_{ex}}(\mathrm{t}) - \left(\mathrm{f_v}(\dot{\mathrm{z}}(\mathrm{t})) + \mathrm{R_U}(\mathrm{t})\right)\dot{\mathrm{z}}(\mathrm{t}) - \left(\mathrm{f_p}(\mathrm{z}(\mathrm{t})) + \mathrm{S_U}(\mathrm{t})\right)\mathrm{z}(\mathrm{t}) - \mathrm{C_r q_r}(\mathrm{t})\right) \\ \dot{\mathrm{q}}_\mathrm{r}(\mathrm{t}) = \mathrm{A_r q_r}(\mathrm{t}) + \mathrm{B_r}\dot{\mathrm{z}}(\mathrm{t}) \end{cases} \tag{3}$$

Where $f_v(\dot{z}(t))$ and $f_p(z(t))$ are defined as follows:

$$\begin{cases} \mathrm{f_v}(\dot{\mathrm{z}}(\mathrm{t})) = \mathrm{R_{loss}} + 0.5\,\rho\,\mathrm{A_w}\,\mathrm{C_d}\,|\dot{\mathrm{z}}(\mathrm{t})| \\ \mathrm{f_p}(\mathrm{z}(\mathrm{t})) = \mathrm{S_b} + \mathrm{S_{rs}} + 2\mathrm{S_m}\left(1 - \mathrm{l_m}/\sqrt{\mathrm{l_m^2} + \mathrm{z}(\mathrm{t})^2}\right) \end{cases} \tag{4}$$

The dynamic structure of a point absorber WEC is shown in Fig. 2, considering the input and output forces.

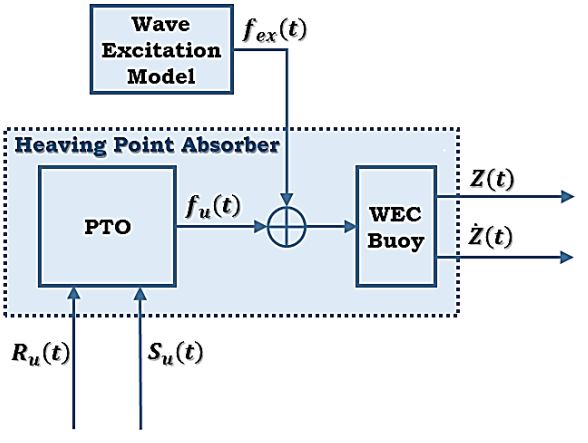

Fig. 1. Dynamic structure of a point absorber WEC.

3. COMPENATING DYNAMIC EFFECTS OF SOME COMPLEX NONLINEAR TERMS IN DYNAMIC MODEL

For harnessing the maximum power and compensating for the complex nonlinear dynamics, the following lemma is introduced.

Lemma: In a point absorber WEC with the following dynamic model [21]

$$\ddot{\mathrm{z}}(\mathrm{t}) = \frac{1}{\mathrm{m}+\mathrm{m}_\infty}\left[\mathrm{f_{ex}} + \mathrm{f_u} - \mathrm{C_r q_r}(\mathrm{t}) - (\mathrm{S_b} + \mathrm{S_{rs}})\mathrm{z}(\mathrm{t}) - \mathrm{R_{loss}}\dot{\mathrm{z}}(\mathrm{t}) - 2\mathrm{S_m}\left(1 - \mathrm{l_m}\sqrt{\mathrm{l_m}^2 + \mathrm{z}(\mathrm{t})^2}\right)\mathrm{z}(\mathrm{t}) - 0.5\,\rho\,\mathrm{A_w}\,\mathrm{C_d}\,|\dot{\mathrm{z}}(\mathrm{t})|\dot{\mathrm{z}}(\mathrm{t})\right], \tag{5}$$

And considering the external force for nonlinear waves, we have:

Now, the control signal can be expressed according to the model in Eq. 7.

$$\begin{cases} R_U(t) = -(R_{loss} + 0.5\,\rho\,A_w\,C_d\,|\dot{z}(t)|) - u_R(t) \\ S_U(t) = -\left(S_b + S_{rs} + 2S_m\left(1 - l_m/\sqrt{l_m^2 + z(t)^2}\right)\right) - u_S(t) \end{cases} \quad (7)$$

After eliminating the dynamic effects of some complex terms, the reduced model of the proposed design can be written as follows:

$$\begin{cases} \ddot{z}(t) = M^{-1}\left(f_{ex}(t) + u_R(t)\dot{z}(t) + u_S(t)z(t) - C_r q_r(t)\right) \\ \dot{q}_r(t) = A_r q_r(t) + B_r \dot{z}(t) \end{cases} \quad (8)$$

The state vector is represented by Eq. 10:

$$x(t) = [z(t),\ \dot{z}(t),\ q_r(t)^T]^T \quad (9)$$

$$\begin{cases} \dot{x}(t) = Ax(t) + Bf_{ex}(t) + B\theta(t) \\ y(t) = Cx(t) \end{cases} \quad (10)$$

$$\theta(t) = u_S(t)z(t) + u_R(t)\dot{z}(t)$$

$$A = \begin{bmatrix} 0_{1\times1} & 1 & 0_{1\times4} \\ 0_{1\times1} & 0_{1\times1} & -M^{-1}C_r \\ 0_{4\times1} & B_r & A_r \end{bmatrix}$$
$$B = [0_{1\times1} \quad M^{-1} \quad 0_{1\times4}]^T \quad (11)$$
$$C = [0_{1\times1}\ 1 \quad 0_{1\times4}]$$

Fig. 3 shows the structure of a point absorber WEC after implementing the compensator:

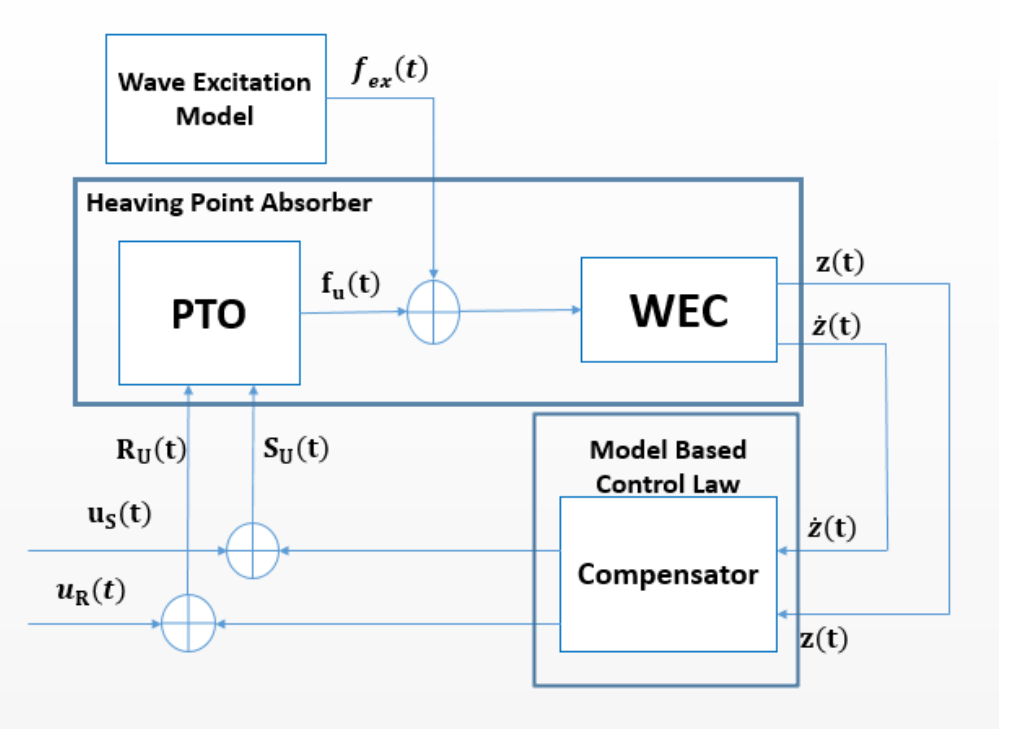

Fig. 2. Structure of point absorbing WEC after implementing compensator.

Given the structure of point absorber WECs, there are uncertainties in the dynamics of these systems. One of these uncertainties is the state variables measurement, which is related to inappropriate performance of water level and wave velocity sensors due to the critical sea conditions, humidity and different weather conditions.

Water-formed scale deposits and the attachment of marine mussels under the buoy over time can be considered as the second uncertainty in the buoy mass.

The uncertainty in the buoy mass can be modeled in a general form as follows:

$$\begin{cases} \ddot{z}(t) = \left(M^{-1} + \widetilde{M^{-1}}\right)\begin{pmatrix} f_{ex}(t) + \left(u_R(t) + d_R(t)\right)\left(\hat{\dot{z}}(t) + \tilde{\dot{z}}(t)\right) \\ +\left(u_S(t) + d_S(t)\right)\left(\hat{z}(t) + \tilde{z}(t)\right) - C_r q_r(t) \end{pmatrix} \\ \dot{q}_r(t) = A_r q_r(t) + B_r\left(\hat{\dot{z}}(t) + \tilde{\dot{z}}(t)\right) \end{cases} \quad (12)$$

Where $\widetilde{M^{-1}}$ is the uncertainty in the buoy mass; $\tilde{\dot{z}}(t)$ and $\tilde{z}(t)$ are the uncertainties in measuring the state variables; $d_R(t)$ and $d_S(t)$ are the uncertainties in measuring the control signals. Furthermore, the total uncertainty was extracted from Eq. (12) and represented by d_{Lumped} or lumped uncertainty.

$$\begin{cases} \ddot{z}(t) = M^{-1}\left(f_{ex}(t) + u_R(t)\dot{z}(t) + u_S(t)z(t) - C_r q_r(t) + d_{Lumped}\right) \\ \dot{q}_r(t) = A_r q_r(t) + B_r \dot{z}(t) + d_q \end{cases} \quad (13)$$

For more precise tracking control and smoother control signal, an IT2FLC is proposed.

.

4. DESIGNING INTERVAL TYPE-2 FUZZY CONTROLLER

After simplifying the proposed model, an IT2FLC is designed to effectively deal with uncertainties and obtain a computationally less complex system than conventional T2FLCs.

$$\begin{aligned} \ddot{z}(t) &= M^{-1}\left(u_R(t)\dot{z}(t) + u_S(t)z(t) \right. \\ &\quad \left. + f_{ex}(t) - C_r q(t)\right) \\ f_{ex}(t) &= 2R_r V_r(t) \end{aligned} \quad (14)$$

The purpose of designing the IT2FLC is to increase power extraction and decrease the velocity tracking error, which is expressed as follows:

$$E = V_r - \dot{z}, \quad \dot{E} = \dot{V}_r - \ddot{z} \quad \rightarrow \quad \dot{E} + \lambda E = 0 \quad \rightarrow \quad \dot{V}_r + \lambda E = \ddot{z} \quad (15)$$

By inserting Eq. (14) into Eq. (15), we have

$$\dot{V}_r + \lambda(V_r - \dot{z}) = M^{-1}\begin{pmatrix} u_R(t)\dot{z}(t) + u_S(t)z(t) \\ +2R_r V_r(t) - C_r q(t) \end{pmatrix}$$

$$M\dot{V}_r(t) + (\lambda M - 2R_r)V_r(t) - \lambda M\dot{z}(t) + C_r q(t) = u_R(t)\dot{z}(t) + u_S(t)z(t) \quad (16)$$

Where $M\dot{V}_r(t) + (\lambda M - 2R_r)V_r(t)$ can be calculated based on the desired velocity, $\lambda M\dot{z}(t)$ can be measured and $C_r q(t)$ can be approximated. The right hand side of Eq. (16) can also be obtained using an IT2FLC.

In the present study, an IT2FLC is proposed for adjusting the values of the new control signals, $u_S(t)$ and $u_R(t)$. The most important advantage of IT2FLC over conventional fuzzy logic controllers is the controller output and the smoothness of the response, besides fewer design parameters [22] .

In the present study, it is proposed that each membership function of IT2FLC (fuzzy set) is the combination of two Gaussian functions with similar center of gravity and variance. These membership functions show the upper and lower boundaries of the T2F interval. The upper limit is unity, while the lower limit should be determined as the third design parameter. The difference between the upper and lower limit is called the footprint of uncertainty. The antecedent membership functions can be determined by a vector of three real parameters (Fig. 4):

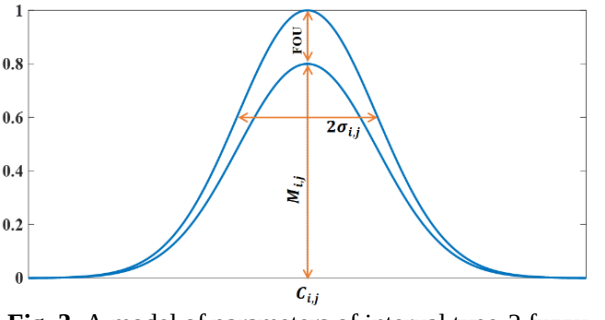

Fig. 3. A model of parameters of interval type-2 fuzzy membership functions.

Additionally, there are two parameters for the output of each fuzzy rule. Therefore, the parameter vector for each fuzzy rule can be written as follows:

$$P_i = [[\sigma_{i,1} \quad C_{i,1} \quad M_{i,1}] \quad \ldots \quad [\sigma_{i,n} \quad C_{i,n} \quad M_{i,n}] \quad [\underline{Y}_i \quad \overline{Y}_i]] \quad (17)$$

Where $\sigma_{i,j}, C_{i,j}$ and $M_{i,j}$ are, respectively, the variance, center, and the upper limit of the Gaussian membership function (Fig. 4) for the *jth* variable input from the *ith* fuzzy rule. Two IT2F systems u_S and u_R are introduced to provide new control signals.

The first IT2F system, which provides the u_S signal, is the buoy displacement represented by z as the only input data. The input vectors for the second IT2F, which provide the u_R signal include the buoy displacement z and ż as well as the excitation force f_{ex}. In other words, the first IT2FLC is single-input single-output, the membership function of each input has three unknown parameters and each output has two unknown parameters, so there are five unknown parameters in total for this system. We consider eight rules for each controller, making a total of 40 unknown parameters for the first fuzzy system. Moreover, in the second IT2FLC, by considering three inputs and one output, there are 88 unknown parameters. Accordingly, a total of 128

parameters are adjusted by the optimization algorithm for each controller.

In the consequent part or output of fuzzy rules, there is two fuzzy variables for the upper and lower limits, and the rule structures for the first and second controllers are as follows:

F z is μ_z^L, THEN u_S is μ_s^L

IF z is μ_z^L, AND ż is μ_{dz}^L, AND f_{ex} is μ_f^L, THEN u_R is μ_R^L (18)

Where, μ_z^L is an interval type-2 fuzzy membership function for the Lth rule of the displacement input or Z. Other member functions can be introduced in a similar way. The operator AND does the multiplication operation in the structure of the rules. Finally, in type-2 fuzzy calculations, the antecedent and consequent have two values for the upper and lower limit in the proposed IT2FLC. To reduce the type, a more efficient and faster algorithm, known as the enhanced iterative algorithm with stop condition, which was first introduced in Ref. [4], is used instead of the KM algorithm. A type-2 fuzzy system can be defuzzified as follows:

$$y = \frac{y_l + y_r}{2} \quad (19)$$

Where, y output is equal to u_r for the first interval type-2 fuzzy system and equal to u_s for the second interval type-2 fuzzy system. Finally, the structural details of the IT2FLC proposed in this paper are presented in Table 2

Table 1. General structure of the proposed interval type-2 fuzzy logic controller.

Total number of unknown parameters	Number of rules	Number of parameters in each rule	Unknown parameters	Output	Input	Controller
40	**8**	**5**	$\sigma_{i,j}$, $C_{i,j}$, $M_{i,j}$	u_S	**Z**	**IT2FLC1**
88	**8**	**11**	$\sigma_{i,j}$, $C_{i,j}$, $M_{i,j}$	u_R	**Z,Ż,** f_{ex}	**IT2FLC2**

5. OPTIMIZING DESIGN PARAMETERS

The adjustment of the proposed IT2FLC parameters, including the fuzzy membership functions parameters, is difficult especially if the trial-and-error method is used. Therefore, we use improved black hole algorithm to adjust the controller parameters.

$$\min(ISE) = \min(\int_0^{t_f} [\dot{Z}_r(t) - \dot{Z}(t)]^2) \quad (20)$$

5.1. Evaluation criterion

In the algorithm of the designed system, the evaluation criterion is the difference between the mean square errors of the output and reference velocities.

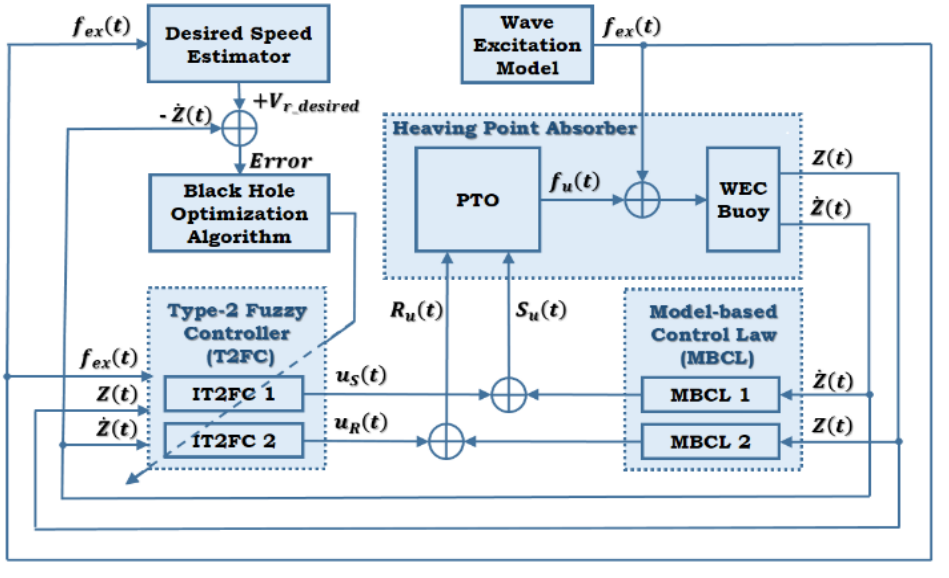

Fig. 4. The Proposed structure for increasing power extraction using black hole optimization.

As can be seen in Fig. 5, the optimal buoy velocity is obtained from the excitation force, and the error is calculated by subtracting the optimal buoy velocity from the actual buoy velocity. The black hole optimization algorithm adjusts the type-2 fuzzy system parameters to reduce the tracking error and increase the power extraction from the sea waves.

6. WAVE SPECTRUM MODEL OF PERSIAN GULF

Standard models are usually related by simple relationships to the measured field data in a certain study. These relationships are expressed using the basic knowledge of irregular waves. Standard spectral wave models at some point regardless of the wave direction are often expressed with the following equation [23].

$$S(f) = \frac{A}{f^5}\exp(-\frac{B}{f^4}) \quad (21)$$

Where, f is the frequency and A and B are constant values. Depending on the model, these constants may be wave elevation, peak period or average period or another parameter. Choosing the standard spectral model depends on the characteristics of the region under study. According to the geographical data from the Persian Gulf and the surrounding coastal lands, the following wave spectrum can be used [23].

$$S_J(\omega) = \frac{\alpha g^2}{\omega^M}\exp\left(-\frac{M}{N}\left(\frac{\omega_P}{\omega}\right)^N\right)\gamma^{\exp\left(\frac{-\left(\frac{\omega}{\omega_p}-1\right)^2}{2\sigma^2}\right)} \quad (22)$$

Where

$$= \begin{cases} 0.07 & if\ \omega < \omega_p \\ 0.09 & if\ \omega \geq \omega_p \end{cases}$$

$$M = 5\ , N = 4$$

$$\alpha \approx 5.061\frac{H_{m0}^2}{T_P^4}\{1\text{-}0.287\ln(\gamma)\} \quad (23)$$

A standard value for γ is 3.3. However, a more appropriate formula for obtaining $H_{m0}$and $T_p$via γ is given as follows:

$$\gamma = exp\left\{3.484(1-0.1975)\left(0.036-\frac{0.0056T_P}{\sqrt{H_{m0}}}\right)T_P^4/H_{m0}^2\right\} \quad (24)$$

Where, $1 \leq \gamma \leq 7$. This range for γ is based on deep-water wave data from the Persian Gulf.

The relationship between peak period and zero-crossing period can be approximated as follows:

$$T_{m02} \approx T_P/(1.30301 - 0.01698\gamma + 0.12102/\gamma) \quad (25)$$

7. SIMULATION

This section reviews the simulation results in three stages. The first stage investigates the performance of the designed controller, the second stage investigates the proposed optimization algorithm and compares it with other algorithms, and the third stage compares the proposed IT2FLC, a T1FLC and a fuzzy sliding mode controller. Finally, the designed controller is implemented and evaluated in the simplified point absorber WEC with compensator in the open waters of the Persian Gulf. The simulation results show the high capacity of power extraction of the open waters of the Persian Gulf.

7.1. Performance analysis of the proposed method

The purpose of optimization is to find the best acceptable solution, considering the constraints and requirements of the problem. Fig. 6 shows the mean performance of the black hole optimization algorithm in 200 iterations, where cost means the mean square of the velocity tracking error.

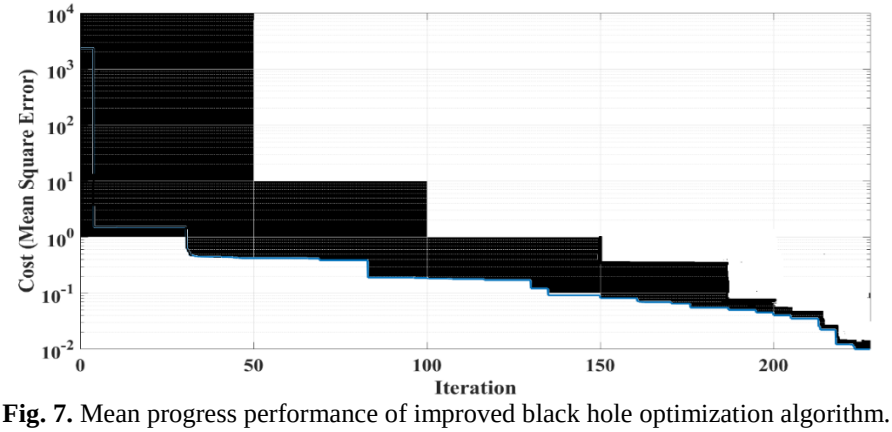

Fig. 7. Mean progress performance of improved black hole optimization algorithm.

To investigate different waveforms, Table 3 presents different Persian Gulf states; by simulating the wave spectrum, the curves of these states are shown in Fig. 7.

Table 3. Different Persian Gulf states.

(H_s) Elevation(m)	($2\pi / \omega_m$) Period(sec)	Sea State
0.3	6.3	1
0.9	7.5	2
1.9	8.8	3
3.3	9.7	4
5.0	12.4	5

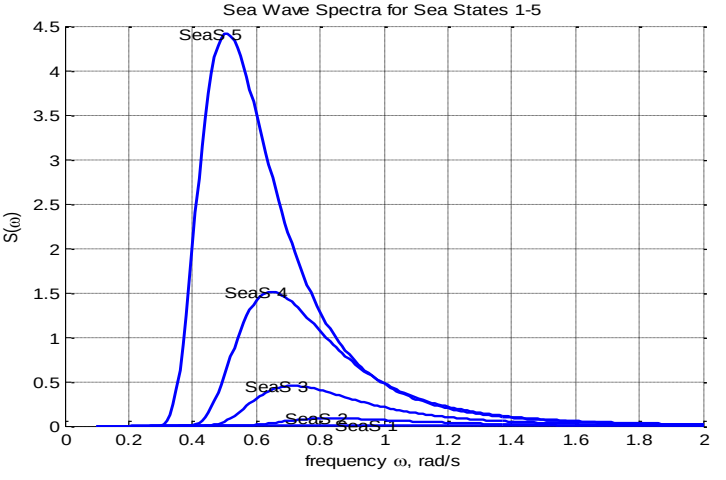

Fig. 7. Persian Gulf states with different wave elevation.

To evaluate the performance of the controller, one of the sea modes has been selected ,the simulation result of sea wave elevation is shown in Fig. 8.

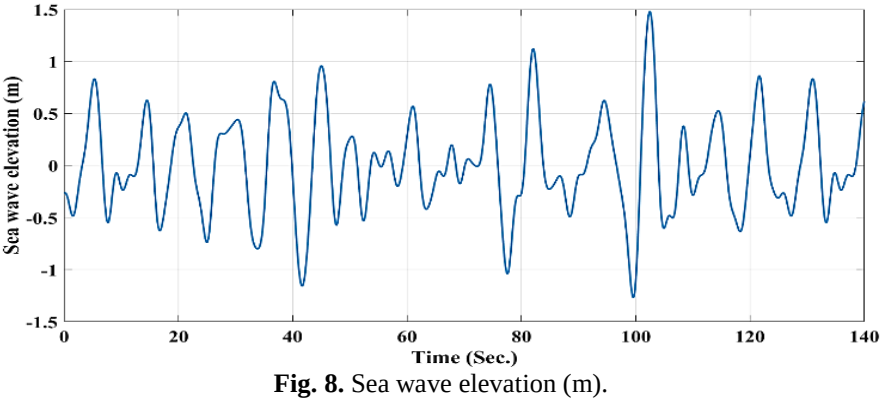

Fig. 8. Sea wave elevation (m).

Sea waves have very complex nonlinear patterns and for maximum power extraction from them, a point absorber control is required. After optimizing, the optimal values of the two controllable parameters of the point absorber, i.e., spring stiffness coefficient and damping coefficient, are added to the system.

As a result, Fig. 9 shows the buoy displacement.

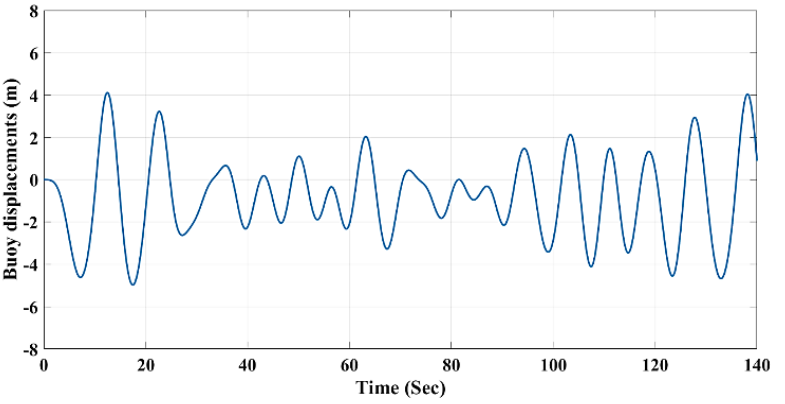

Fig. 9. Buoy displacement (m).

According to this figure, the buoy displacement has a smooth curve, which matches the boundaries. Fig. 10 shows the buoy velocity.

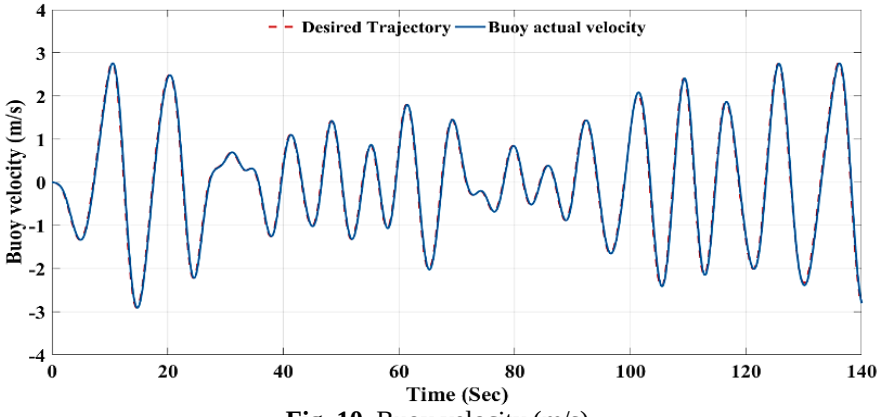

Fig. 10. Buoy velocity (m/s).

The optimum designed velocity can be calculated using the excitation force. Moreover, if the optimum and the actual velocities of the buoy are tracked, the absorbed power will be maximized. From Fig. 10, the performance of velocity tracking based on the proposed method is acceptable (the mean square error of velocity tracking is 8.17e-8). The maximum power absorption and its average over time are shown in Fig. 11.

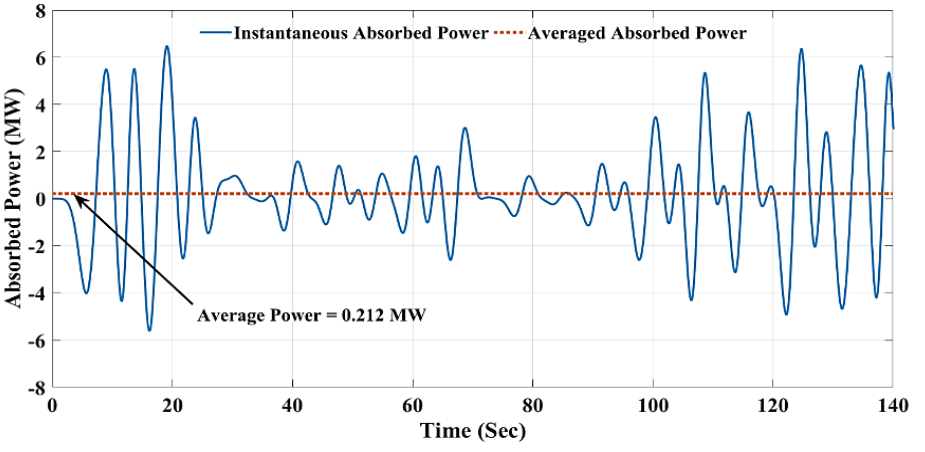

Fig.11. Absorbed power.

According to this figure, the average absorbed energy reaches 212 kW after 140 seconds.

To maximize the power absorption of the system, the stiffness and damping coefficients are adjusted by the fuzzy system. Figs. 12 and 13 show the variations of, respectively, stiffness and damping coefficients of the PTO.

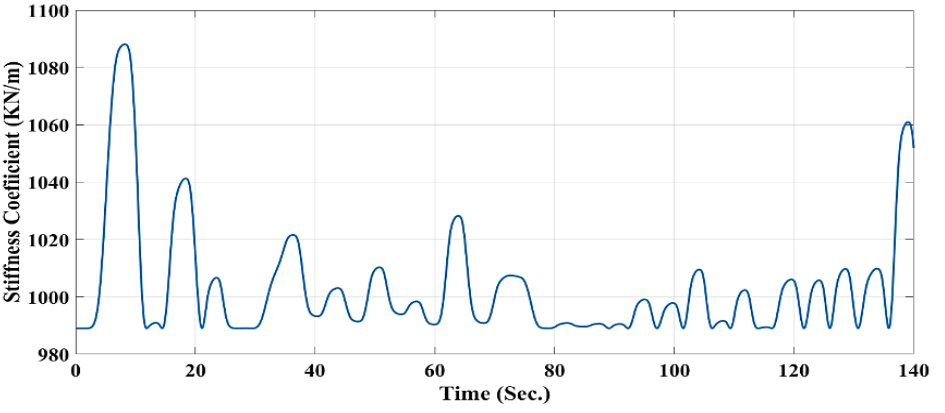

Fig.12. PTO stiffness coefficient.

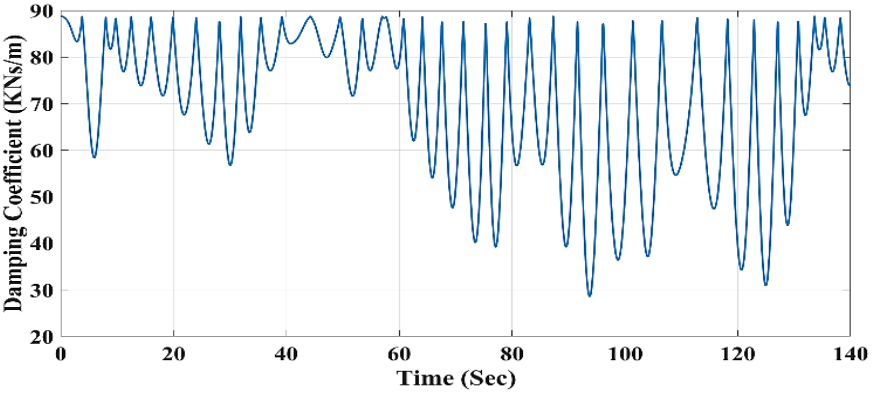

Fig. 13. PTO damping coefficient.

The stiffness and damping coefficients are determined based on the PTO characteristics over certain a range [24] . The force from PTO is shown in Fig. 14, where the maximum power extraction can be determined.

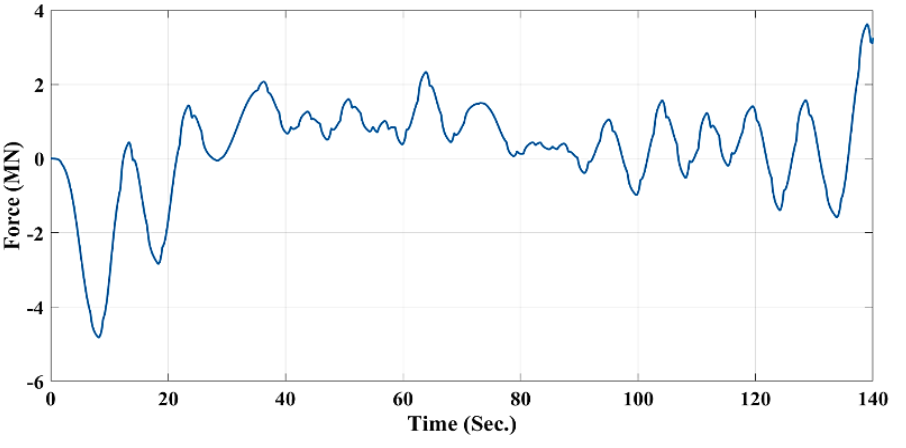

Fig. 14. Force exerted by PTO.

7.2. Comparing the Proposed Method with Other Methods

Before implementing the controller, the wave excitation force is applied to the point absorber WEC. As shown in Fig. 15, and using the power maximization theorem [25] for WECs, the actual buoy velocity ($\dot{z}$) and the desired wave velocity ($\dot{z}_r$) are not in phase before the implementation of the controller, so the desired velocity and actual buoy velocity are not tracked.

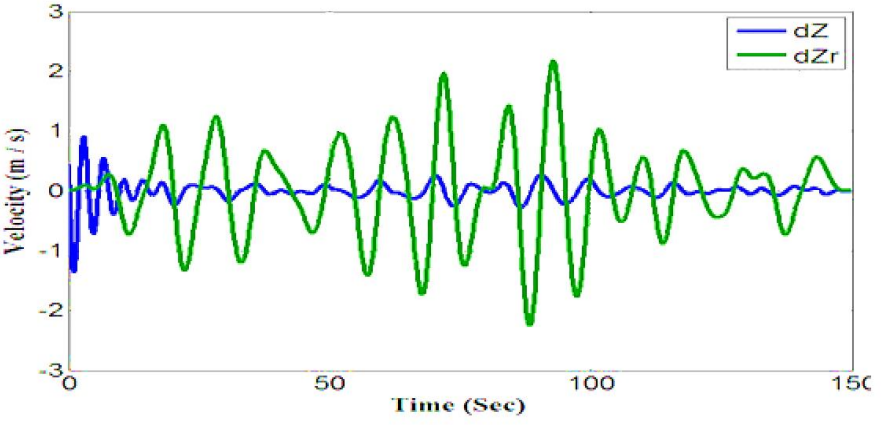

Fig. 15. Actual and optimum velocities before implementing the controller.

According to Fig. 16, the IT2FLC with the improved black hole algorithm can track the reference velocity faster and better than with the conventional black hole and PSO algorithms. From Fig. 16, the error of the conventional fuzzy controller is higher than that of the proposed method. Therefore, the efficiency of the proposed method is considerable.

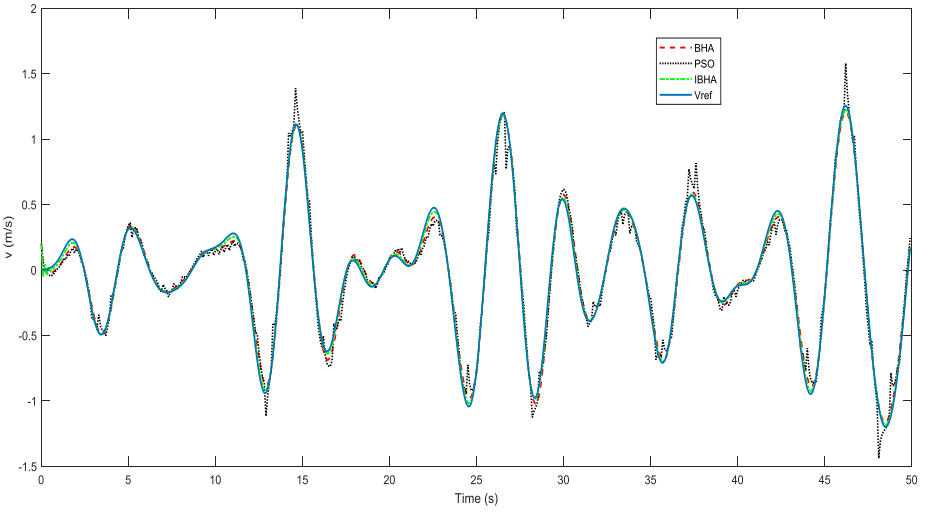

Fig.16. Comparison of reference velocity tracking using T2FLC adjusted by IBHA, PSO algorithm and BHA.

$f_u(t)$ is the input force, which acts on the WEC through the PTO with the purpose of extracting the maximum power, as a controlling effort by the proposed system. Fig. 17 illustrates the PTO force, which is controlled by the T2FLC and its membership function parameters are adjusted by the improved black hole algorithm. Furthermore, a comparison with PSO and conventional black hole algorithms is presented in this figure.

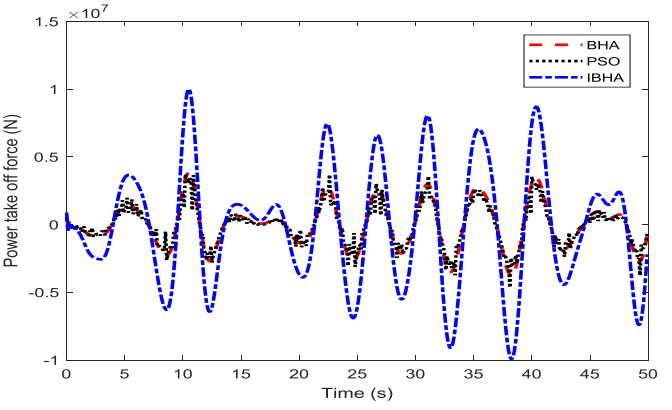

Fig. 17. Comparison of PTO force using T2FLC adjusted by IBHA, PSO algorithm and BHA.

In the proposed method, the maximum input force generates more power. In Figs. 18 and 19, the power extracted and the energy absorbed by the WEC system under T2FLC with turbulent BH algorithm are compared to those with BH, firefly, and PSO algorithms.

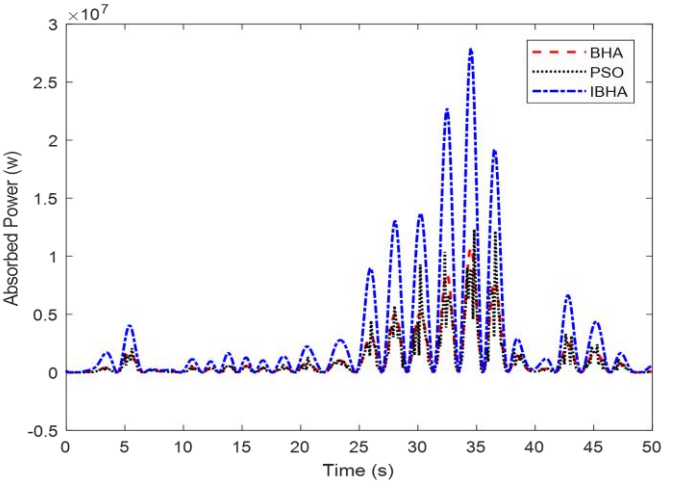

Fig. 18. Comparison of power absorbed by WEC.

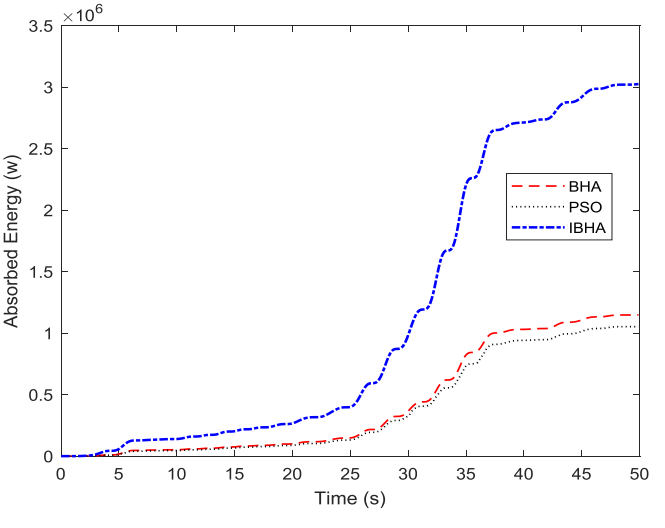

Fig. 19. Comparison of energy absorbed by WEC.

In Ref [21, 23], Jama et al. introduced a fuzzy controller to extract maximum power from a point absorber WEC, in which the membership functions are adjusted using the PSO algorithm. Moreover, in Ref. [26], a hybrid control structure including a sliding mode controller and a reference trajectory generator was introduced. The results of these two references are compared with the proposed method in the same conditions. In this problem, there are two control signals, i.e., the spring stiffness and damping coefficients of the PTO to control and maximize power extraction. Therefore, these two signals are first compared. In Ref [21], the calculations of these two control outputs and their values are not reported. Consequently, in Figs. 20 and 21, the damping and stiffness coefficients are only compared with Ref. [26]

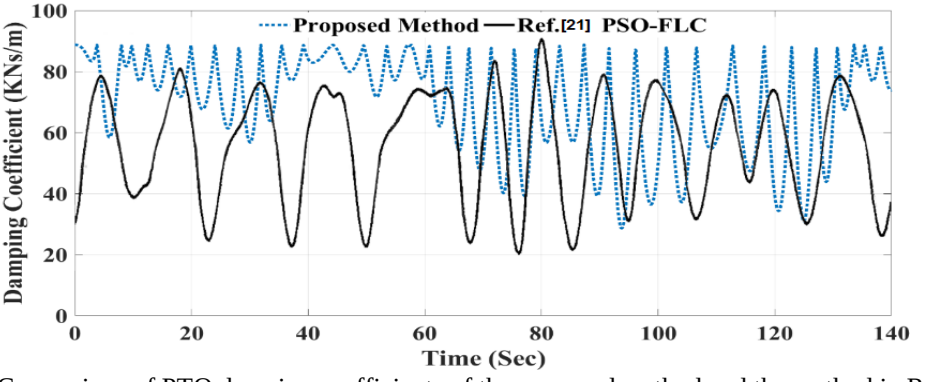

Fig. 20. Comparison of PTO damping coefficients of the proposed method and the method in Ref. [8].

According to Fig. 20, in the proposed method, the damping coefficient is more sensitive to the velocity tracking error. Additionally, from Fig. 21, the stiffness coefficient of the proposed controller is much smoother but over a higher range of values. The force generated by the PTO is shown in Fig. 22.

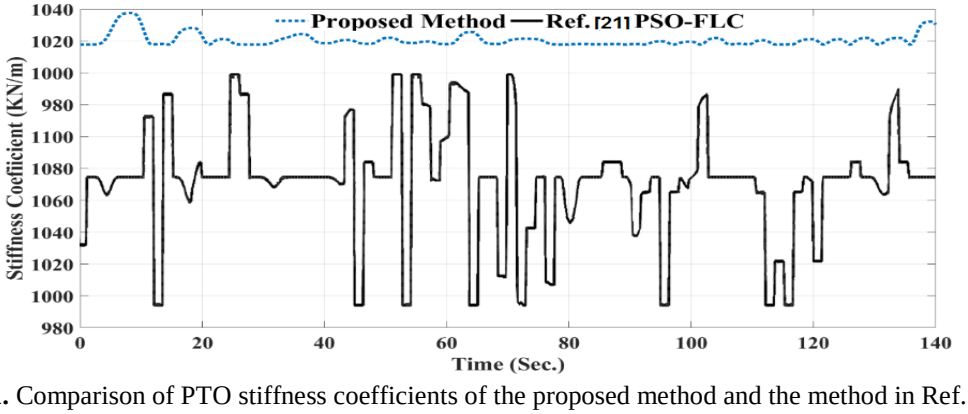

Fig.21. Comparison of PTO stiffness coefficients of the proposed method and the method in Ref. [8].

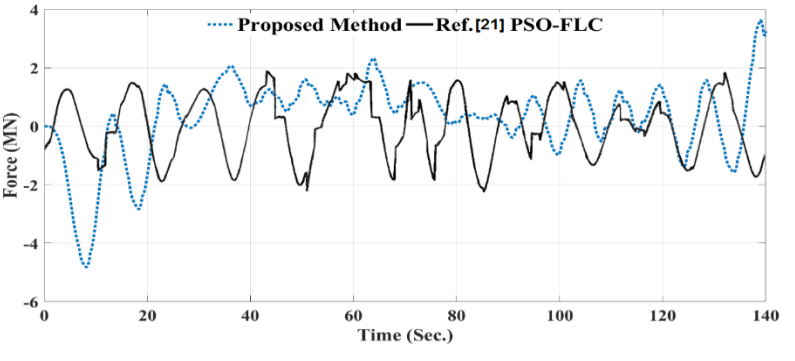

Fig. 22. Comparison of power generated by PTO system in the proposed method and the method in Ref [35].

As shown in Fig. 22, the PTO force generates more peaks in the proposed method. In Table 4, the average power absorbed by the proposed method is compared with that by the methods of Refs. [27]and [7].

Table 4. Comparison of generated power.

Proposed method	HCS [27]	PSO-FLC [21]	Methods
212 KW	166 KW	72 KW	Average power absorption over 140 seconds

According to Table 4, the proposed method has a superior performance.

7.3. Studying the Proposed Controller in Persian Gulf Waters

Wave elevation values are given in Table 5, according to 12-year modeling of the results of limit analysis in the Persian Gulf and deep waters. Using the wave elevation and period over a long time, the energy density spectrum of the waves can be calculated by the relationships expressed for the Persian Gulf waves. Fig. 23 shows the spectra of the Persian Gulf waves.

Table 5. Limit analysis in the Persian Gulf [31].

Period (year)	Wave elevation	Waves period
2	**2.82**	6.72
5	**3.62**	7.61
10	**4.15**	8.15
20	**4.67**	8.64
50	**5.33**	9.23
100	**5.83**	9.66
200	**6.32**	10.66

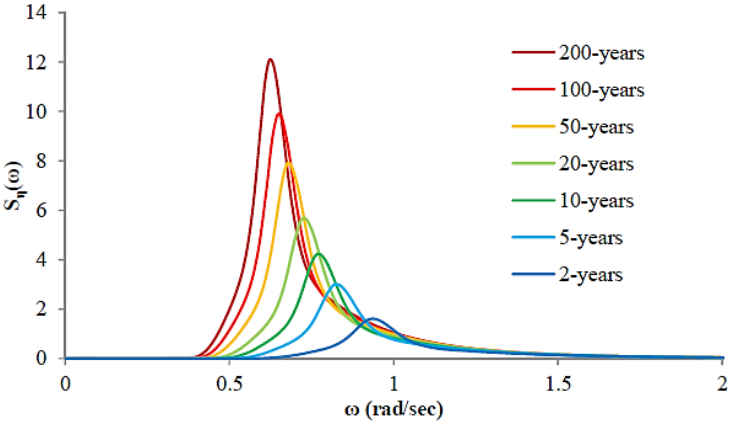

Fig. 23. Persian Gulf wave spectra.

In the simulation of the fuzzy controller for the energy converter of irregular waves in the Persian Gulf, the proposed method is used to minimize the error between the reference velocity and the actual buoy velocity. Therefore, the power extracted from the irregular waves is maximized. Here the proposed turbulent black hole algorithm is used to minimize the time integral of the absolute value of the error. The simulation results for irregular waves with Jonswap spectrum versus time are shown in Fig. 24.

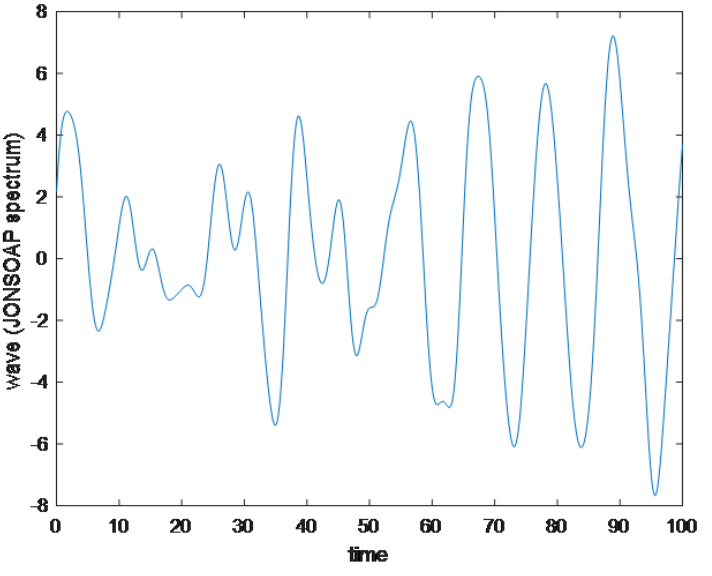

Fig. 24. Irregular Jonswap wave spectrum in terms of time.

Fig, 25 shows the reference velocity and the buoy velocity in terms of time for the Persian Gulf waves. It is clear that the reference velocity has been tracked with a slight discrepancy.

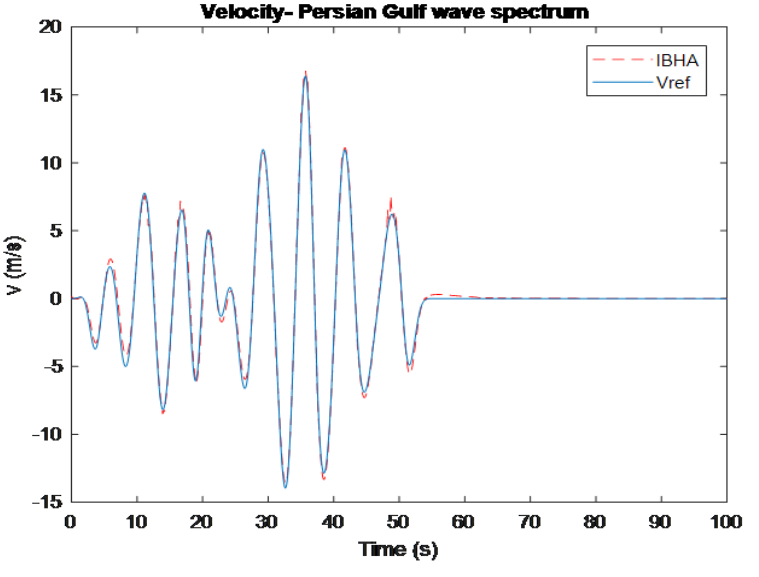

Fig. 25. Reference velocity and the velocity from the buoy versus time for the Persian Gulf waves.

Figs. 26 and 27 show, respectively, the power and energy curves in terms of time for the Persian Gulf waves. According to Fig. 26, 391 kW electricity can be extracted from the waves.

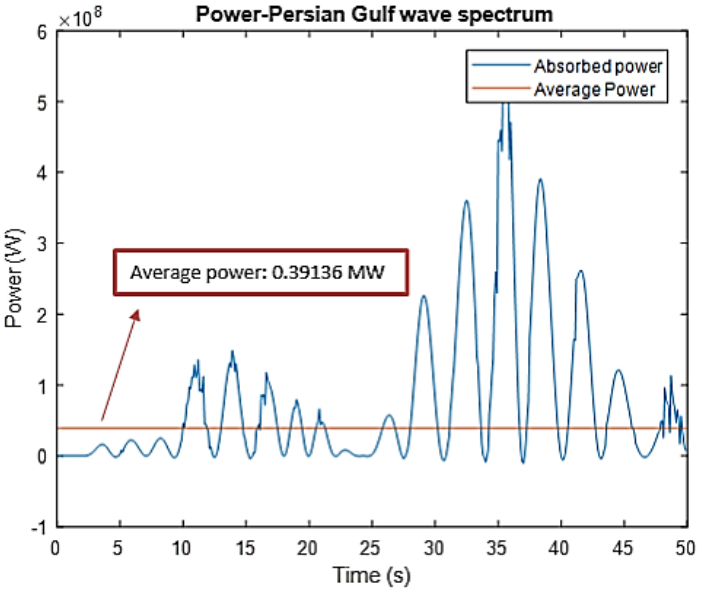

Fig. 26. Extracted power versus time for the Persian Gulf wave spectrum.

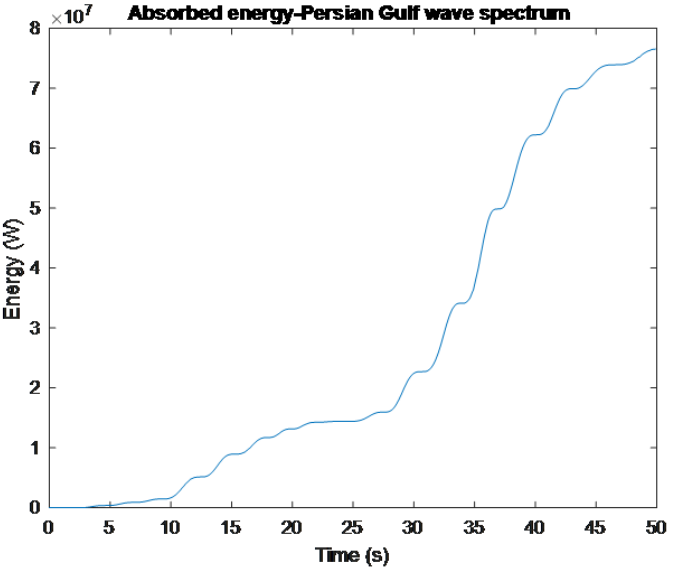

Fig. 27. Absorbed wave energy versus time for the Persian Gulf wave spectrum.

8. DISCUSSION

The main contribution of this paper is to use a type 2 fuzzy controller to extract maximum power from a WEC point absorber. Another part of this paper is the study of different wave states related to the Persian Gulf using the proposed controller. The results showed that the performance of buoy velocity chase using the proposed method is acceptable. The absorbed power sample was obtained by adjusting the damping and stiffness coefficients using the proposed type 2 fuzzy controller. An improved black hole algorithm was used to adjust the damping coefficients, hardness and type 2 fuzzy controllers. In order to evaluate the proposed method, the results were compared with conventional particle mass optimization algorithms and black holes. The results showed that in pursuing speed and power extraction, the proposed method performed better than the other two methods. Also, the results comparison to similar research shows the superiority of the proposed method in higher power extraction compared to previous

research. Finally, the proposed controller in different states of the Persian Gulf wave was investigated. The results showed that this controller is able to extract the maximum power in the Persian Gulf wave.

9. CONCLUSION

In this paper, a new interval type-2 fuzzy logic controller was designed to extract maximum power from sea waves using a point absorber. To optimize the type-2 fuzzy weights, a black hole optimization algorithm was used. Since a point absorber is a complex nonlinear system, a new strategy was proposed to compensate for the closed-loop nonlinear relationships for modeling and reducing the complexities. Using this compensation strategy, the black hole algorithm was able to optimize the interval type-2 fuzzy parameters for maximum power extraction. To verify the performance and efficiency of the proposed algorithm, some simulations were performed. The simulation results confirmed the high performance and efficiency of the proposed design. Finally, the wave spectrum of the Persian Gulf was studied, and the proposed method was implemented on it. Moreover, the power extracted from the Persian Gulf waves was determined and the high energy capacity of these waves was demonstrated to be of great importance for generating electricity in the country. In future studies, the authors would like to investigate the maximum power extraction from the sea waves using a type-2 fuzzy neural-network control scheme combined with the proposed structure or any other type-reduction method. Additionally, for extending this research work, some other measures can also be used, such as considering the effects of measurement noise, including more uncertainties and implementing an array of WECs, to extract more power.

REFERENCES

[1] P. Melin, **"Emanuel Ontiveros-Robles ,Claudia I. Gonzalez , An approach for parameterized shadowed type-2 fuzzy membership functions applied in control applications,"** *Soft Computing*, Vol. 23(11), pp. 3887-3901, 2019.

[2] Sepúlveda R., Montiel-Ross O., Castillo O., Melin P, **"Embedding a KM Type Reducer for High Speed Fuzzy Controller into an FPGA,"** *Soft Computing in Industrial Applications*, Vol. 75. Springer, pp. 217-228, 2010.

[3] Hagras, Hani, **"Type-2 Fuzzy Logic Controllers: A Way Forward for Fuzzy Systems in Real World Environments,"** *Computational Intelligence*, Vol. 5050, pp. 181-200, 2008.

[4] Mendel, J. M., "J. M. Mendel, ``**On KM algorithms for solving type-2 fuzzy set problems,"** Fuzzy Syst, Vols. 21, No. 3, pp. 426-446, Jun. 2013.

[5] Mendel, D. Wu and J. M**., "Enhanced Karnik-Mendel algorithms,"** *IEEE Trans. Fuzzy Syst*, Vols. 17, No. 4, pp. 923-934, Aug. 2009..

[6] X. Liu, J. Mendel, and D. Wu, **"Study on enhanced Karnik-Mendel algorithms: Initialization explanations and computation improvements,"** *Inf. Sc*i, Vols. 184,No. 1, pp. 75-91, 2012.

[7] P. Melin ; O. Castillo, **"Intelligent control of non-linear dynamic plants using type-2 fuzzy logic and neural networks,"** *in 2002 Annual Meeting of the North American Fuzzy Information Processing Society Proceedings*. NAFIPS-FLINT 2002 (Cat. No. 02TH8622), New Orleans, LA, USA, USA, February 2002.

[8] J. Li, R. John, S. Coupland, and G. Kendall**, "On Nie-Tan operator and type-reduction of interval type-2 fuzzy sets,"** *IEEE Trans. Fuzzy Syst*, Vol. Apr. 2018, pp. 1036-1039, 26, No. 2.

[9] D. Sun, Q. Liao, X. Gu, C. Li and H. Ren, **"Multilateral Teleoperation With New Cooperative Structure Based on Reconfigurable Robots and Type-2 Fuzzy Logic,"** *IEEE Transactions on Cybernetics*, Vols. 49, no. 8, no. doi: 10.1109/TCYB.2018.2828503, pp. 2845-2859, Aug. 2019.

[10] Emanuel Ontiveros,Robles PatriciaMelin, **"A hybrid design of shadowed type-2 fuzzy inference systems applied in diagnosis problems,"** *Engineering Applications of Artificial Intelligence*, Vol. 86, pp. 43-55, November 2019.

[11] D.Wang, Y. Chen and**, "Study on centroid type-reduction of general type-2 fuzzy logic systems with weighted enhanced Karnik-Mendel algorithms,"** *Soft Comput*, Vols. 22, No. 4, pp. 1361-1380, Feb. 2018..

[12] D, Wu, **"Approaches for reducing the computational cost of interval type-2 fuzzy logic systems: overview and comparisons,"** *IEEE Trans Fuzzy Syst*, Vol. 2, p. 80–99, 2013.

[13] F. Chao, D. Zhou, C. Lin, L. Yang, C. Zhou and C. Shang, **"Type-2 Fuzzy Hybrid Controller Network for Robotic Systems,"** *IEEE Transactions on Cybernetics*, no. doi: 10.1109/TCYB.2019.2919128, pp. 2168-2267, 2019.

[14] Bayram, H. Dalman and M., **"Interactive Fuzzy Goal Programming Based on Taylor Series to Solve Multiobjective Nonlinear Programming Problems With Interval Type-2 Fuzzy Numbers,"** *IEEE Transactions on Fuzzy Systems*, Vols. 26, No. 4, no. doi: 10.1109/TFUZZ.2017.2774191, pp. pp. 2434-2449, Aug. 2018.

[15] M. Han, K. Zhong, T. Qiu and B. Han, "**Interval Type-2 Fuzzy Neural Networks for Chaotic Time Series Prediction: A Concise Overview,"** *IEEE Transactions on Cybernetics*, Vols. 2720-2731, no. doi: 10.1109/TCYB.2018.2834356, pp. 2720-2731, 49, no. 7.

[16] J. Huang, M. Ri, D. Wu and S. Ri**, "Interval Type-2 Fuzzy Logic Modeling and Control of a Mobile Two-Wheeled Inverted Pendulum,"** *IEEE Transactions on Fuzzy Systems*, Vols. 26, No. 4, no. doi: 10.1109/TFUZZ.2017.2760283, pp. 2030-2038, Aug. 2018.

[17] E.Anderlini, D.I.M. forehand, E. Bannon , M. Abusara, **"Reactive control of a wave energy converter using**

artificial neural network," *marine energy*, Vol. 19, pp. 207-220, 2017.

[18] Xuanrui Huang, Kai Sun, Xi Xiao, , **"A Neural Network-based Power Control Method for Direct-Drive Wave Energy Converters in Irregular Waves,"** *ieee Transactions on Sustainable Energy*, pp. 1940-3022, 2020.

[19] Ning Wang , Yusen Jia and Shui Fu, **"Spring-resonance-assisted maximal power tracking control of a directdrive wave energy converter,"** *Transactions of the Institute* of, 2121.

[20] Yao Zhang, Peter Stansby, Guang Li **, "Non-causal Linear Optimal Control with Adaptive Sliding Mode Observer for Multi-Body Wave Energy Converters,"** *IEEE Transactions on Sustainable Energy*, pp. 1949-3029, 2020.

[21] Mohammed Jama, Addy Wahyudie , Ali Assi and Hassan Noura, **"An Intelligent Fuzzy Logic Controller for Maximum Power Capture of Point Absorbers,"** *Energies*, pp. 4033-4053, 2014.

[22] Li, G., & Belmont, M. R., **"Model predictive control of sea wave energy converters–Part I: A convex approach for the case of a single device,"** *Renewable Energy*, Vol. 69, pp. 453-463, 2014.

[23] V. jahanmard, M.A dastan, "**Generate record time history of waves based on the range obtained from the limit conditions of the Persian Gulf region in the return period,"** *in oic*, tehran, 2013.

[24] Zhan, S., He, W., & Li, G. **, "Robust feedback model predictive control of sea wave energy converters,"** *IFAC-PapersOnLine*, Vol. 50, pp. 141-146, 2017.

[25] MM Aman, GB jasmon, AHA Bakar, **"optimum network reconfiguration based on maximiation of system loadability using continuation power flow teoream,"** *international journal of electrical power & energy system*, Vol. 54, pp. 123-133, 2014.

[26] Zhan, S., Huijberts, H., Na, J., & Li, G**., "Optimal controller design and constraints analysis of a sea wave energy converter,"** *In 2016 UKACC 11th International Conference on Control (CONTROL)*, pp. 1-6, 2016.

[27] Fusco, F., & Ringwood, J. V., **"A study of the prediction requirements in real-time control of wave energy converters,"** *IEEE Transactions on Sustainable Energy*, Vol. 3(1), pp. 176-184, 2011.

[28] Chen, Y**., "Study on Sampling Based Discrete Nie-Tan Algorithms for Computing the Centroids of General Type-2 Fuzzy Sets,"** *in IEEE Access*, vol. vol. 7, pp. 156984-156992, 2019.

[29] NguyenAnh, MukeshPrasad, Narasimalu Srikanth, SureshSundaram, **"Wave Forecasting using Meta-cognitive Interval Type-2 Fuzzy Inference System,"** *Procedia Computer Science*, Vol. 144, pp. 33-41, 2018.